Hydrogen Recovery Analyses Based on LOGSIG Activation Functions in Feedforward Neural Networks

Maimunatun Nawar Mohd Yazan[1], Ashraf Azmi[1], Muhammad Azan Tamar Jaya[2], Mohd Roslee Othman[3], Illi Khairunnisa binti Shamsudin[3] and Iylia Idris[1*]

[1] School of Chemical Engineering, College of Engineering, Universiti Teknologi MARA, 40450 Shah Alam, Selangor, Malaysia
[2] Kolej GENIUS Insan, Universiti Sains Islam Malaysia, 71800 Nilai, Negeri Sembilan, Malaysia
[3] School of Chemical Engineering, Universiti Sains Malaysia, 14300 Nibong Tebal, Pulau Pinang, Malaysia

iyliaidris@uitm.edu.my

Abstract. Hydrogen is a crucial intermediate product that is widely used in the petrochemical and oil sectors. Efficiently improving hydrogen recovery technology is crucial for achieving sustainable success and fulfilling environmental obligations, given the increasing demand for hydrogen and the growing urgency of environmental concerns. To solve this issue, a Feedforward Artificial Neural Network (FANN) model was developed to predict and improve the amount of hydrogen gas that can be made from palm kernel shell activated carbon (PKS-AC) syngas production. The study used 60 experimental data points to examine the impact of adsorption processes, such as adsorption, pressure equalisation, desorption, and re-pressurisation modes, on hydrogen recovery through pressure swing adsorption procedures. The optimisation process was performed using the MATLAB (R2017b) software, specifically the Neural Network (NN) tool, with a dataset containing adsorption pressure, duration of adsorption and blowdown time data. The study demonstrated that using the LOGSIG activation function achieved the smallest mean square error (MSE) of 0.00010 when 19 hidden neurons were utilised. The regression coefficients (R) for training, validation, and testing were 0.91598, 0.99042, and 0.91718, respectively. The utilisation of this model has the potential to facilitate the development of cost-effective and efficient designs for on separation of pressure swing adsorption processes.

Keywords: Hydrogen, Palm Kernel Shell, Activated Carbon, Feedforward, Artificial Neural Networks, PSA.

© The Author(s) 2024
N. A. S. Abdullah et al. (eds.), *Proceedings of the International Conference on Innovation & Entrepreneurship in Computing, Engineering & Science Education (InvENT 2024)*, Advances in Computer Science Research 117,
https://doi.org/10.2991/978-94-6463-589-8_36

1 Introduction

Recovery of hydrogen from syngas is a crucial step in utilizing this versatile fuel for various applications like clean power generation and fuel cell technology. Syngas is a byproduct of gasification processes such as coal gasification, biomass gasification, and natural gas reforming. It is mainly composed of hydrogen, carbon monoxide and carbon dioxide. There are several methods for recovering hydrogen; pressure swing adsorption (PSA), membrane separation, and cryogenic distillation are a few of them, each with pros and cons of its own. However, hydrogen gas recovery from syngas using PSA with activated carbon is a proven and effective method [1].

CO is extremely toxic while CO_2 is greenhouse gas allegedly contributes to global warming [2]. As a result, removing these gases and recovering hydrogen is an essential approach for cutting down on waste and air pollution in the environment. By capturing hydrogen before it is released into the atmosphere, air quality is improved, emissions are avoided, and the environmental impact is decreased [3].

Pressure swing adsorption (PSA) is a low-cost substitute for conventional absorption methods in the cyclic adsorption process used for gas separation and purification. A PSA process's primary feature is its ability to alternate between adsorption and desorption by varying the system pressure. The PSA process is run in cyclic steady state (CSS) for applications. The performance of PSA systems can be influenced by the number of adsorption beds, bed dimensions, layers, cycle configuration, and operating conditions [4], [5].

Fig. 1 shows a two-bed PSA unit's basic operation. Adsorbent, purge valves, and valves are the main components of the equipment that control the cyclic process by making use of the different pressure settings.

In chemical processes, an artificial neural network (ANN) is a valuable tool for accurately assessing the relationship between system inputs and outputs through its layers and nodes. Consequently, ANNs have been widely used in various areas of chemistry, including process simulation and control, adsorption and reaction kinetics and reducing computational costs [6]. ANNs can be regularly updated with new data, allowing them to adapt to changing environmental and operational conditions. This updatability makes ANNs an invaluable tool for maintaining excellent hydrogen recovery performance over time. [7].

Hence, the research aims to achieve three primary objectives: forecasting the quantity of hydrogen gas obtained by using an Artificial Neural Network (ANN) and experimental data; projecting the recovery of hydrogen by altering factors including adsorption pressure, adsorption time, and blowdown time using logsig activation function. For the purpose of comparing experimental and predicted data, Multilayer feedforward artificial neural networks (FANN) were implemented using MATLAB™ (R2017b) guidelines.

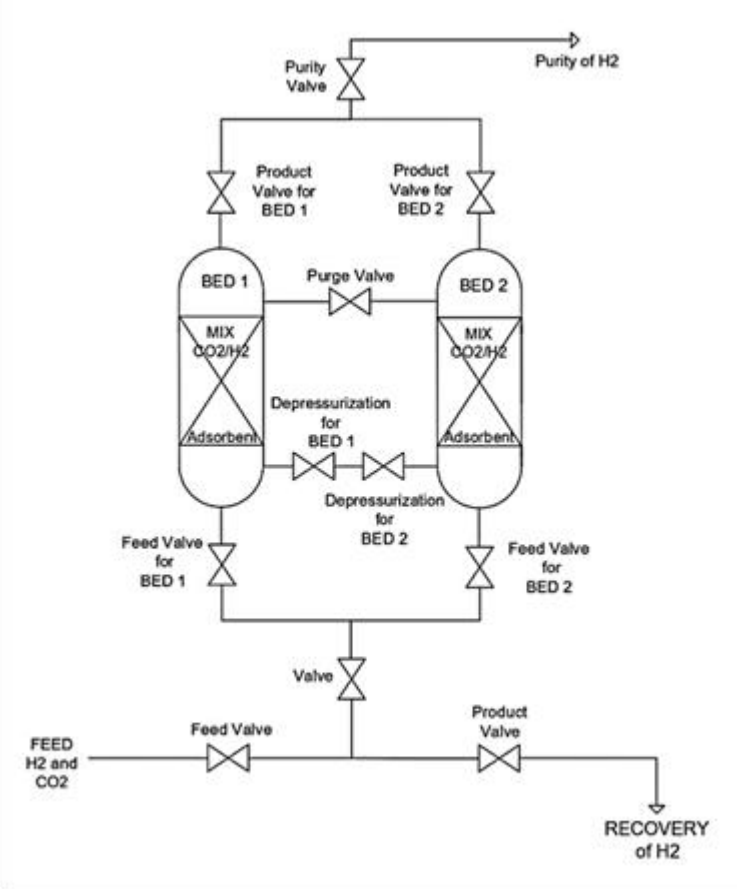

Fig. 1. PSA unit used in recovery of hydrogen [8].

2 Methodology

2.1 Modelling recovery of hydrogen using Feedforward Artificial Neural Network (FANN)

Forecasting the prediction of hydrogen recovery from a pressure swing adsorption process using the MATLAB™ R2017b neural network toolbox. The objective of this modelling is to forecast the hydrogen recovery from PSA in the gasification process. The study utilised the feed forward back propagation neural network (FANN) algorithm, which is considered the most appropriate method for solving fitting problems, particularly in mapping input and output. The input and output data sets utilised in this modelling analysis were obtained from prior experimental work conducted in this research. The input data for the ANN modelling consisted of feed adsorption time, adsorption pressure, and blowdown time. The output data, used for training,

testing, and validation, was the recovery of hydrogen obtained from experimental study.

The performance of the predicted output from the Artificial Neural Network (ANN) was evaluated using the Mean Square Error (MSE) value and the regression value (R). These values were obtained from the constructed model while comparing the predicted values with the experimental values. The trial-and-error method was utilized to select the optimal network structure, based on the lowest Mean Squared Error (MSE) value and the R value closest to 1, for the testing, validation, and training datasets. The process of trial and error involves experimenting with different combinations of hidden nodes and layers to identify the optimal number of neurons and hidden layers needed for the artificial neural network (ANN) architecture.

2.2 Artificial neural network (ANN) model development

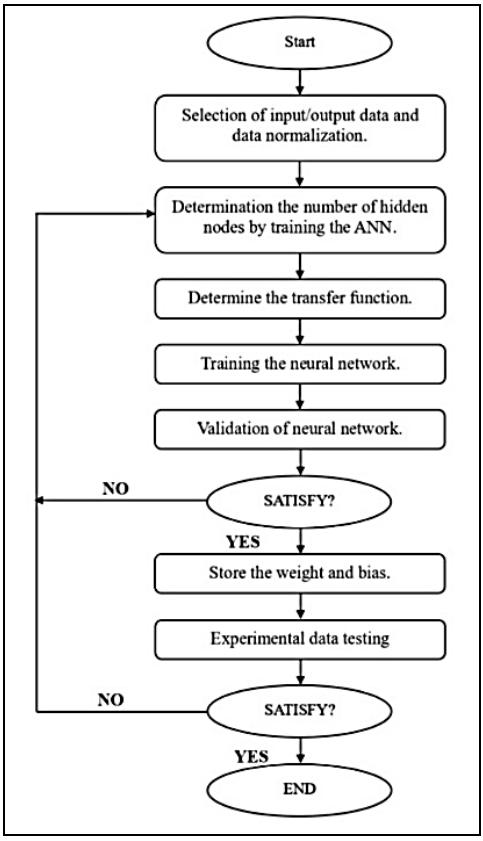

Fig. 2. The illustration was used to model feed-forward artificial neural networks (FANNs) (Idris et al., 2019b).

To predict the outcome of the modelling process, the adsorption pressure was held constant at 2 bars. The network model was developed by selecting the network type, the number of layers, the number of neurons in the hidden layer, the training function, and the transfer functions for the hidden and output layers.

The flowchart for feed forward artificial neural network (FANN) modeling is presented in **Fig. 2**. A feedforward neural network, characterized by its unidirectional flow of data through circular connections between its nodes, represents the fundamental type of the neurol network chosen in this study. In this model, data moves exclusively in one direction, never reversing or looping back [9].

2.2.1 Neural network structure

The neural network structure has been categorised into two types: feedforward network and feedback network [10]. In a feedback network, the data or information is acquired from the output of the preceding levels. The flow of data or information between neurons occurs through the input-output connections of different neuronal layers. A feedforward network is commonly referred to as a multi-layer perceptron (MLP). The choice of using a feedforward network is based on its simplicity and ability to prevent over-parameterization [11]. Furthermore, the weight and bias are appropriately modified during the training procedure, enabling the network to accurately forecast the output for a given set of inputs. A neural network layer consists of three distinct layers: the input layer, the hidden layer, and the output layer.

2.2.2 Data size structure

For a neural network to operate well and achieve generalisation, the right data size must be chosen during training. Apparently, there is no single approach for assessing the quantity of the data for adequate network training [11], [12]. In this study, the input data was randomly divided into three separate data sets. The first set, comprising 70% of the data, was used for training and consisted of 42 samples. The second set, accounting for 15% of the data, was used for validation and contained 9 samples. The remaining 15% of the data, also consisting of 9 samples, was used for testing.

2.2.3 Selection of neural network model

2.2.3.1 *Network type*

There are many different kinds of artificial neural networks, but one of the simplest ones is called a feedforward neural network. Within this network, information flows only in a unidirectional manner, progressing from the input nodes, passing via any hidden nodes, and ultimately reaching the output nodes. The network is acyclic. Feedforward neural networks were the first type of artificial neural network

developed and are less complex compared to other types such as recurrent neural networks and convolutional neural networks [13].

2.2.3.2 *Number of hidden layers*

The hidden layer serves as an intermediary layer positioned between the input and output layers of the network. The number of hidden layers in the network varies depending on the problem. Certain situations require a single hidden layer, while others necessitate numerous hidden layers. Hidden layers consist of a group of compact neurons that transmit data from the training layer to other layers [14]. When dealing with actual-world issues using a multilayer feed-forward network, it is crucial to take into account the size of the hidden layer [15]. The optimal artificial neural network (ANN) architecture can be determined by carefully choosing the number of neurons in the hidden layer. By increasing the number of neurons in the hidden layer, the model can effectively represent the training data. However, there is still a chance that it may fail to accurately represent data that falls outside of the training range. To accomplish this, one neuron is used as an initial guess, followed by an increase in the number of neurons one at a time [11].

2.2.3.3 *Number of hidden neurons*

Typical guidelines show the number of hidden neurons that should be between the size of the input layer and the size of the output layer [16]. As per Vujičić et al., 2016, the quantity of hidden neurons must not exceed twice the size of the input layer. The training algorithm was optimised by determining the most suitable number of hidden layers for the constructed artificial neural network (ANN) model. There is no singular approach to ascertain the ideal number of hidden neurons. This work utilised the technique of expanding the neural network, where the training process begins with a limited number of hidden neurons.

As the error is determined, the number of neurons may be increased throughout the operation. The chosen number of hidden neurons was determined by a trial-and-error process, based on the outcomes of the error function with regard to the training data set for MSE, aiming to reach a value closest to 0 [18]. This is the standard approach used to select the appropriate number of hidden neurons. The initial selection of the number of hidden neurons is often equal to the number of input neurons or nodes in the network.

In order to accomplish this, an initial estimate is made using three neurons in the hidden layer, and then the number of neurons is gradually increased from 1 to 20. If the initial number of hidden neurons fails to yield a high correlation coefficient value and a minimal MSE, then the number of neurons is raised. But, as the number of concealed neurons incorporated in the model increases, the model's complexity also increases. Once the number of hidden layers and the number of hidden neurons

has been determined, the Artificial Neural Network (ANN) is prepared for training [11].

2.2.3.4 Selection *of training algorithm*

The Levenberg-Marquardt (LM) algorithms were utilized in learning, prediction, classification, optimization, control, and detection [19]. They were also used for classification. Given their extensive applicability, Levenberg-Marquardt algorithms were a suitable substitute for artificial neural network learning in hydrogen recovery optimization. LM method is widely used because to its excellent convergence speed and stability while training artificial neural network (ANN) models [20]. This step is necessary to ascertain the suitable weight and bias values and to achieve the optimal network structure. The Levenberg-Marquardt (LM) method is a frequently used optimisation strategy for a range of artificial neural network (ANN) applications, particularly for solving nonlinear least square problems. The training procedure utilising the Backpropagation (BP) method is an iterative optimisation technique that aims to minimise the performance function by appropriately altering the weights and biases of the network. The Mean Squared Error (MSE) is the most commonly used performance metric. Furthermore, this training procedure is used to adjust the network's weight by minimising an objective function, specifically the Mean Squared Error (MSE) between the network's outputs and the desired outputs [11], [21].

3 Results and discussion

3.1 Artificial neural network (ANN) model development

This model severs to aid researchers in predicted hydrogen gas recovery using PSA systems equipped with ANN tools. The study focused on an optimal adsorption pressure of two bar as the specific input pressure range. Adsorption times at the feed inlet were varied between 0.5,1,3, and 5 minutes, while the blowdown time remained constant at 0.5 minutes.

A multilayered feedforward back propagation neural network was implemented in this investigation. Input data included feed inlet pressure, adsorption duration and blowdown time, while the output (target data) was hydrogen recovery based on experimental results. The modelling analysis utilized sixty data samples, with the default configuration of the ANN tool in $Matlab^{TM}$ R2017b employing a training-validation-testing ratio of 70:15:15, respectively

3.1.1 Dataset

The training data were used to generate the network parameters (weights and biases), ensuring the network learned from the dataset. Validation data then verified the flexibility of these parameters. The test dataset provided an unbiased evaluation of

how well the final model fits the training data. **Table 1** presents the actual data used in this ANN modeling experiment.

Usually, ANNs are constructed with only one output neuron. This is applicable for tasks with a solitary goal variable, such as predicting a price, classifying a picture (cat vs dog), or creating a singular value. The presence of two output neurons in this study enables the network to simultaneously predict or classify two distinct yet interconnected variables more accurately [22]. The classification result, in comparison to the regression output, offers a more accurate evaluation of the operational status of hydrogen recovery.

Table 1. Experimental data of hydrogen recovery.

Experimental Data				
Input			**Output**	
Pressure (bar)	**Adsorption time (min)**	**Blowdown time (min)**	**C1**	**C2**
Training Set				
2	0.5	0.5	0.03	0.25
2	0.5	0.5	0.19	0.26
2	0.5	0.5	0.19	0.25
2	0.5	0.5	0.26	0.25
2	0.5	0.5	0.25	0.25
2	0.5	0.5	0.26	0.25
2	0.5	0.5	0.25	0.25
2	0.5	0.5	0.26	0.25
2	0.5	0.5	0.25	0.25
2	0.5	0.5	0.25	0.25
2	0.5	0.5	0.24	0.25
2	0.5	0.5	0.24	0.25
2	0.5	0.5	0.26	0.25
2	0.5	0.5	0.26	0.25
2	0.5	0.5	0.25	0.25
2	1.0	0.5	0.09	0.17
2	1.0	0.5	0.18	0.17
2	1.0	0.5	0.18	0.17
2	1.0	0.5	0.18	0.17
2	1.0	0.5	0.18	0.17
2	1.0	0.5	0.20	0.17
2	1.0	0.5	0.18	0.17
2	1.0	0.5	0.18	0.16
2	1.0	0.5	0.17	0.16
2	1.0	0.5	0.17	0.16

2	1.0	0.5	0.15	0.16
2	1.0	0.5	0.17	0.16
2	1.0	0.5	0.16	0.19
2	1.0	0.5	0.16	0.16
2	1.0	0.5	0.17	0.16
2	3.0	0.5	0.02	0.07
2	3.0	0.5	0.08	0.07
2	3.0	0.5	0.08	0.07
2	3.0	0.5	0.08	0.07
2	3.0	0.5	0.08	0.07
2	3.0	0.5	0.07	0.07
2	3.0	0.5	0.07	0.07
2	3.0	0.5	0.07	0.07
2	3.0	0.5	0.07	0.06
2	3.0	0.5	0.07	0.07
2	3.0	0.5	0.03	0.07
2	3.0	0.5	0.07	0.07
		Validation Set		
2	3.0	0.5	0.07	0.07
2	3.0	0.5	0.07	0.06
2	3.0	0.5	0.07	0.07
2	5.0	0.5	0.16	0.44
2	5.0	0.5	0.46	0.41
2	5.0	0.5	0.45	0.31
2	5.0	0.5	0.41	0.40
2	5.0	0.5	0.44	0.42
2	5.0	0.5	0.26	0.45
		Testing Set		
2	5.0	0.5	0.47	0.43
2	5.0	0.5	0.48	0.41
2	5.0	0.5	0.49	0.31
2	5.0	0.5	0.44	0.40
2	5.0	0.5	0.10	0.45
2	5.0	0.5	0.46	0.40
2	5.0	0.5	0.36	0.38
2	5.0	0.5	0.44	0.39
2	5.0	0.5	0.43	0.45

3.1.2 **Network optimization of ANN model**

The neural network proposed in this study was FANN, which utilized the Levenberg-Marquardt (LM) back- propagation training approaches. The study con-

ducted by [23] concluded that the LM or *trainlm* training function was the most effective among all. The logsig or logistic sigmoid function is a mathematical function that transforms the input into a value ranging from 0 to 1. This property makes it particularly suitable for tasks involving binary classification. The earlier work conducted by [24], utilized logistic regression to identify and exclude less significant features. **Table 2** displays the MSE values obtained from the training data set for different numbers of hidden neurons at activation function of Logsig which yielded the lowest MSE value of 0.00010 with 19 neurons, thus giving the most accurate predicted results.

Table 2. MSE value from training data set for a variety of hidden neurons at logsig transfer function.

No. of Hidden Neuron	Model Error (MSE)
1	0.00057
2	0.00079
3	0.00015
4	0.00021
5	0.00017
6	0.00033
7	0.00036
8	0.00030
9	0.00371
10	0.00048
11	0.00353
12	0.00018
13	0.00017
14	0.00027
15	0.00037
16	0.00016
17	0.00039
18	0.00027
19	0.00010
20	0.00037

The mean squared error of the network model decreased as the number of training steps grew, as demonstrated in **Table 3**. However, an overabundance of training might lead to a rise in mistakes. This statement aligns with numerous studies [25]. The training database must be analyzed in order to accurately estimate the number of neurons and hidden layers prior to the neural network design [23].

Table 3. MSE value from training data set for a variety of hidden neurons at logsig transfer function.

No. of times training performed	Activation function	No. of Hidden Neuron	MSE
1st	Logsig	19	0.00048
2nd			0.00014
3rd			0.00011
4th			0.00010

Fig. 3 compares the number of neurons in the hidden layer with the error coverage for the log sigmoid function (LOGSIG). As the number of neurons increased, the error coverage approached zero, indicating that the network could achieve optimal results when using 19 neurons [23]. Throughout alterations in the network architecture, the MSE exhibited fluctuations between its minimum and maximum values. The performance of the neural network was notably affected by changes in the number of hidden layers and the configurations of neurons within those layers [26].

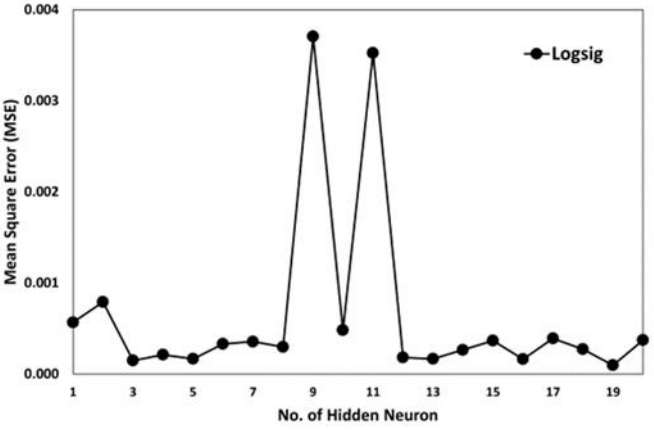

Fig. 3. The effect of hidden layer neuron numbers on MSE and network performance using logsig activation functions.

The selection of the number of neurons in different layers of an artificial neurol network (ANN) is crucial for its successful training. The number of neurons in the input layer is determined by the number of input parameters, while the number in the output layer corresponds to the output parameters. However, the number of neurons in the hidden layer is not predetermined and requires careful consideration. The overall effectiveness of the ANN hinges on its ability to accurately model real-world scenarios through appropriate neural network architecture [26].

In this study, early stopping was used to prevent overfitting as the error value on validation data increased. The optimal number of neurons was determined based on the MSE and R values in the training dataset. Insufficient neurons relative to the complexity of the problem could lead to "underfitting". Conversely, an excessive number of neurons might cause "overfitting", which could significantly degrade the network's performance [14].

3.1.3 Performance of the developed ANN model

After training a network, a simulation was conducted to evaluate its performance on new, previously unseen data—an essential step to gauge how well the network generalizes to unfamiliar inputs. Using a feedforward backpropagation multilayer neural network with the Levenberg- Marquardt training algorithm, minimal MSE and maximal correlation coefficient R were achieved for the dataset.

The activation function played a crucial role in neural networks by determining whether a neuron should be activated based on the weighted sum plus bias. It introduced nonlinearity to the neuron's output, enabling it to handle complex tasks and learn effectively [27]. The performance of the ANN model developed with this activation function is highlighted in this section. **Table 4** presents the characteristics of the model generated in the current study, providing a concise overview of the implementation of the ANN application in MATLAB.

Table 4. Table captions should be placed above the tables.

Characteristics	Commentary
Algorithm	Feed forward back propagation
Minimize error function	MSE
Learning type	Supervised training
Training algorithm	Levenberg-Marquardt
Hidden layer	logistic sigmoid function.
Output layer	Logsig
Number of hidden layers	2
Number of neurons in input layer	3
Number of neurons in hidden layer	19
Number of neurons in output layer	2

Implementing an alternative activation function, logsig, with the smallest MSE value of 0.00010 in the training section, the performance of the adsorption condition in hydrogen recovery is demonstrated. In **Fig. 4**, the scatter regression (R) diagram displays the actual values from the experimental data and the predicted data recovery of hydrogen from the developed ANN model for the training data set. The

experimental results exhibit a strong correlation with the ANN models, as illustrated in **Fig. 5**, with a R value of 0.94700. **Fig. 6** illustrates the comparison of hydrogen recovery values between the experimental data and the predicted results generated by the Artificial Neural Network (ANN) model for the training dataset.

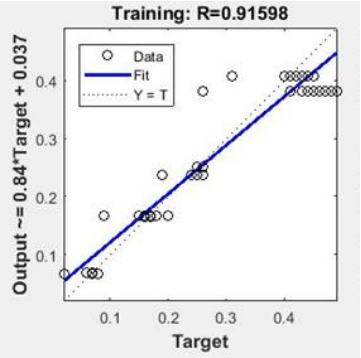

Fig. 4. Scatter regression plot of actual and ANN model's predicted recovery of hydrogen values for training dataset.

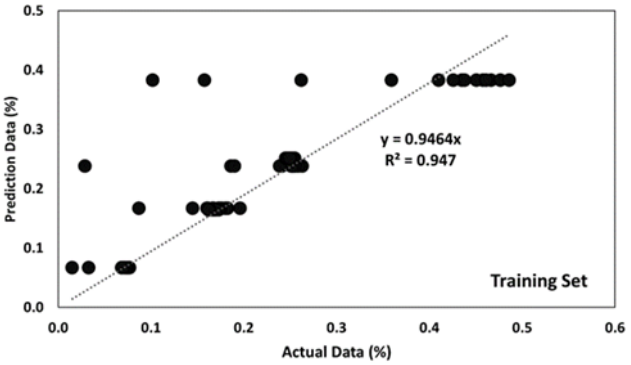

Fig. 5. A correlation coefficient between the actual and the predicted hydrogen recovery for training dataset.

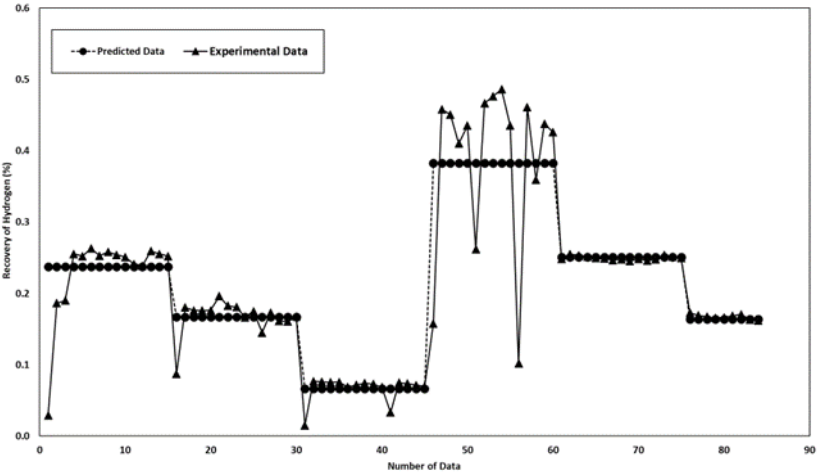

Fig. 6. Comparison of the recovery of hydrogen between the experimental values and the predicted values obtained from ANN model for training data set.

Fig. 7 illustrates the actual and predicted hydrogen recovery values for the validation data set in a scatter chart. The validation procedure yielded an impressive R value of 0.99042. The hydrogen gas recovery values derived from the experimental study are compared to those predicted by the ANN model for the validation data set in **Fig. 8**, with a correlation coefficient value (R) of 0.97440. **Fig. 9** represents the comparison of the recovering hydrogen values between the experimental values and the predicted numbers that were developed from the artificial neural network model for the validation data set.

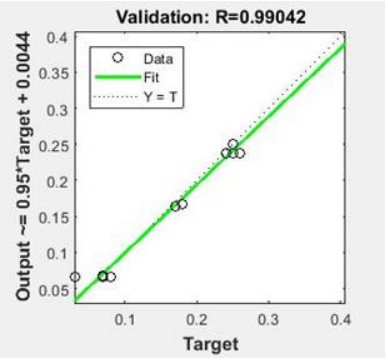

Fig. 7. Scatter regression plot of actual and ANN model's predicted recovery of hydrogen values for validation dataset.

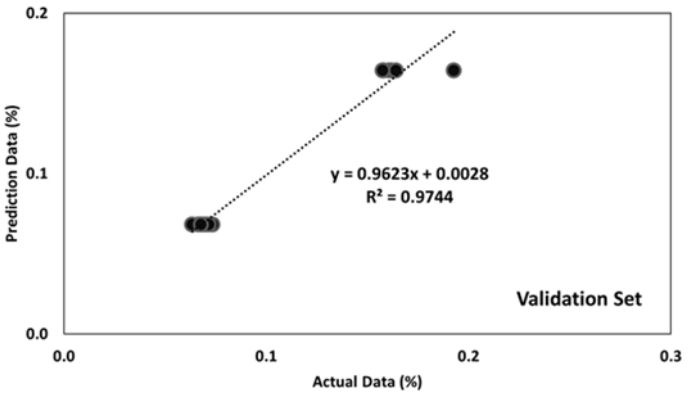

Fig. 8. A correlation coefficient between the actual and the predicted hydrogen recovery for validation dataset.

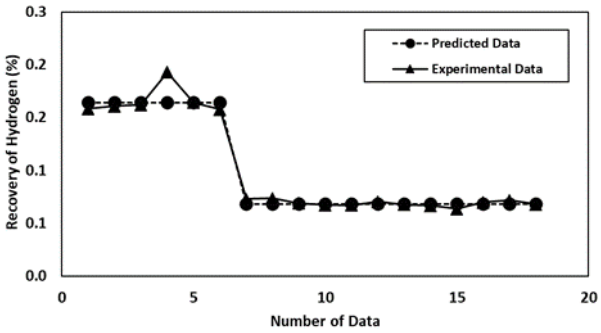

Fig. 9. Comparison of the recovery of hydrogen between the experimental values and the predicted values obtained from ANN model for validation data set.

A scatter plot of the experimental data versus the predicted particle size data is provided in **Fig. 10** to assess the accuracy of the developed ANN model. The R value of 0.91728 indicates that the results derived from the testing data set were highly acceptable. The comparison of hydrogen recovery values between the experimental and predicted values derived from the ANN model for the testing data set is demonstrated in **Fig. 11**. The R value of 0.91370 is a satisfactory correlation coefficient between the actual data from the testing set and the predicted hydrogen recovery. **Fig. 12** depicts the comparison of hydrogen recovery values between the experimental and predicted values for the testing data set, as developed from the ANN model.

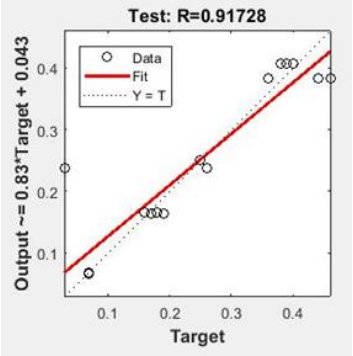

Fig. 10. Scatter regression plot of actual and ANN model's predicted recovery of hydrogen values for testing dataset.

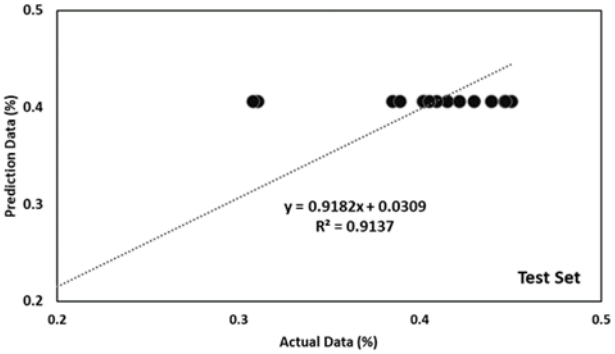

Fig. 11. A correlation coefficient between the actual and the predicted hydrogen recovery for testing dataset.

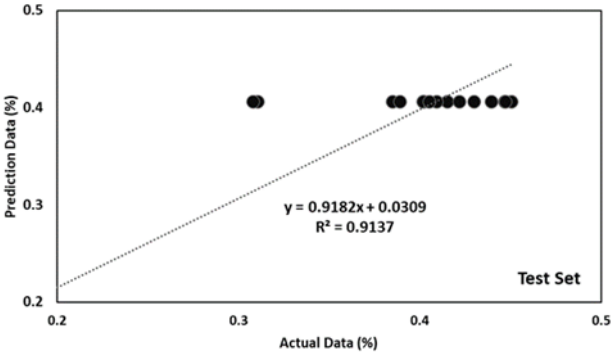

Fig. 12. Comparison of the recovery of hydrogen between the experimental values and the predicted values obtained from ANN model for testing data set.

While **Fig. 13** illustrates a scatter regression plot that integrates the predicted and actual particle size values for overall data points utilized in the log sigmoid function study. The R value of 0.92420 indicates that the model's performance is greatly satisfactory. Lastly, **Fig. 14** illustrates that the ANN model's predicted and experimental hydrogen recovery values for the entire data set resulted in a R value of 0.96210, which is highly satisfactory.

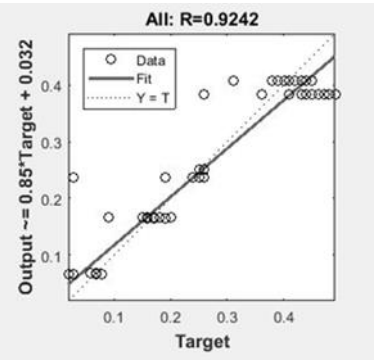

Fig. 13. Scatter regression plot of actual and ANN model's predicted recovery of hydrogen values for overall dataset.

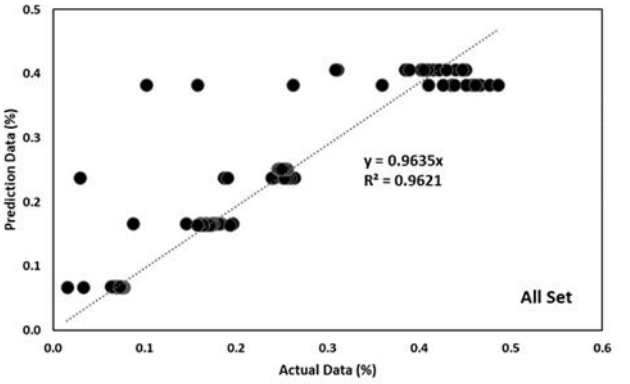

Fig. 14. A correlation coefficient between the actual and the predicted hydrogen recovery for overall dataset.

A neuron's activation function is a critical parameter that significantly impacts the results. Effective outcomes are evidently achieved by selecting the appropriate activation function [28]. The logsig activation function demonstrated superior performance for the ANN model. The results indicated that the ANN model performed poorly in terms of the number of neurons (fewer than five) in all error measurement criteria (in both median and standard deviation). Nevertheless, the median

values exhibited a modest mean square error, indicating that the optimal performance was achieved at approximately 18-19 artificial neurons. As a result, 19 neurons were ultimately selected as the optimal number of neurons for the logsig activation function. In this study, the best neural network model was also the one with the lowest MSE value and the highest R value. This is due to the fact that the R-value is significantly closer to 1 than the other two training algorithms that were evaluated. Additionally, the LM training algorithm has an R-value of 1, indicating that it is the most suitable algorithm, and that the data is well-suited to this model [29]. The logsig function was therefore selected as the optimal function for the recovery of hydrogen [30].

4 Conclusions

The study successfully utilized artificial neural networks on Matlab 2017b to predict hydrogen gas recovery, analysing algorithm function, mean square error, and number of neurons. The feed forward neural network successfully predicted hydrogen gas recovery through a command window. The number of neurons in the hidden layer was varied to train and test a variety of different networks. A three-layer feedforward artificial neural network (FANN) was utilised for modelling purposes. The FANN layer consisted of three input variables, one hidden layer, and one output. A total of 60 experimental data points were included in the model. Various networks were trained and tested by altering the number of neurons in the hidden layer. The regression coefficients (R) were assessed for training, validation, and testing, yielding values of 0.91598, 0.99042, and 0.91728, respectively. The log sigmoid function (logsig) was used with 19 hidden neurons, resulting in a mean square error (MSE) of 0.00010. The developed FANN demonstrated accurate and efficient prediction of the experimental data, achieving a strong overall correlation coefficient of 0.924200 for the three input variables. The FANN model was found to be a valuable tool for determining the effective parameters of the PSA process, as our findings had indicated. By means of estimations for various materials and structures, like a recurrent neural network (RNN), the authors hope to increase the application of the optimal ANN structures in the evaluation of other adsorption parameters in the future. Moreover, the actual number of hidden layers remains a challenging chore. It would be advisable to widen the research going forward to ascertain the precise ideal number of hidden layers.

Acknowledgments. The author(s) gratefully acknowledge the financial support from the College of Engineering, Universiti Teknologi MARA (UiTM), and the provision of experimental data by Universiti Sains Malaysia (USM). This assistance was crucial to the successful completion of this research.

References

[1] J. Lui, W. H. Chen, D. C. W. Tsang, and S. You, "A critical review on the principles, applications, and challenges of waste-to-hydrogen technologies," Dec. 01, 2020, *Elsevier Ltd*. doi: 10.1016/j.rser.2020.110365.

[2] N. Warwick, P. Griffiths, J. Keeble, A. Archibald, and J. Pyle, "Atmospheric implications of increased Hydrogen use," 2022.

[3] A. C. Lewis, "Optimising air quality co-benefits in a hydrogen economy: a case for hydrogen-specific standards for NO x emissions," *Environmental Science: Atmospheres*, vol. 1, no. 5, pp. 201–207, Jul. 2021, doi: 10.1039/D1EA00037C.

[4] R. Zhang, Y. Shen, Z. Tang, W. Li, and D. Zhang, "A Review of Numerical Research on the Pressure Swing Adsorption Process," May 01, 2022, *MDPI*. doi: 10.3390/pr10050812.

[5] D. Stolten and B. Emonts, "Hydrogen Science and Engineering: Materials, Processes, Systems and Technology," 2016.

[6] N. D. Vo, D. H. Oh, J. H. Kang, M. Oh, and C. H. Lee, "Dynamic-model-based artificial neural network for H2 recovery and CO2 capture from hydrogen tail gas," *Appl Energy*, vol. 273, Sep. 2020, doi: 10.1016/j.apenergy.2020.115263.

[7] L. Zhang, H. Li, and X. G. Kong, "Evolving feedforward artificial neural networks using a two-stage approach," *Neurocomputing*, vol. 360, pp. 25–36, Sep. 2019, doi: 10.1016/j.neucom.2019.03.097.

[8] I. Idris, A. Abdullah, I. K. Shamsudin, and M. R. Othman, "Optimizing purity and recovery of hydrogen from syngas by equalized pressure swing adsorption using palm kernel shell activated carbon adsorbent," in *AIP Conference Proceedings*, American Institute of Physics Inc., Jul. 2019. doi: 10.1063/1.5117119.

[9] G. Bilgiç, E. Bendeş, B. Öztürk, and S. Atasever, "Recent advances in artificial neural network research for modeling hydrogen production processes," *Int J Hydrogen Energy*, vol. 48, no. 50, pp. 18947–18977, Jun. 2023, doi: 10.1016/J.IJHYDENE.2023.02.002.

[10] S. D. Al-Majidi, M. F. Abbod, and H. S. Al-Raweshidy, "A particle swarm optimisation-trained feedforward neural network for predicting the maximum power point of a photovoltaic array," *Eng Appl Artif Intell*, vol. 92, p. 103688, Jun. 2020, doi: 10.1016/J.ENGAPPAI.2020.103688.

[11] I. Idris, Z. Ahmad, M. Roslee Othman, F. Sholahudin Rohman, A. Ilyas Rushdan, and A. Azmi, "Application of artificial neural network to predict water flux from pretreated palm oil mill effluent using direct contact membrane distillation," in *Materials Today: Proceedings*, Elsevier Ltd, Jan. 2022, pp. S411–S417. doi: 10.1016/j.matpr.2022.04.084.

[12] B. Eren, R. Ileri, E. Dogan, N. Caglar, and I. Koyuncu, "Development of artificial neural network for prediction of salt recovery by nanofiltration from textile industry wastewaters," *Desalination Water Treat*, vol. 50, no. 1–3, pp. 317–328, 2012, doi: 10.1080/19443994.2012.719743.

[13] K. Xu, M. Zhang, J. Li, S. S. Du, K. I. Kawarabayashi, and S. Jegelka, "How Neural Networks Extrapolate: From Feedforward to Graph Neural Networks," *ICLR 2021* -

9th International Conference on Learning Representations, Sep. 2020, Accessed: Jul. 22, 2024. [Online]. Available: https://arxiv.org/abs/2009.11848v5

[14] M. Uzair and N. Jamil, "Effects of Hidden Layers on the Efficiency of Neural networks," in *Proceedings - 2020 23rd IEEE International Multi-Topic Conference, INMIC 2020*, Institute of Electrical and Electronics Engineers Inc., Nov. 2020. doi: 10.1109/INMIC50486.2020.9318195.

[15] I. Idris, A. Abdullah, I. K. Shamsudin, and M. R. Othman, "Comparative analyses of carbon dioxide capture from power plant flue gas surrogate by micro and mesoporous adsorbents," *J Environ Chem Eng*, vol. 7, no. 3, p. 103115, Jun. 2019, doi: 10.1016/J.JECE.2019.103115.

[16] J. Heaton, "The Number of Hidden Layers," Heaton Research. Accessed: Jan. 09, 2024. [Online]. Available: https://www.heatonresearch.com/2017/06/01/hidden-layers.html

[17] T. Vujičić, T. Matijević, and Z. Ševarac, "Comparative Analysis of Methods for Determining Number of Hidden Neurons in Artificial Neural Network," 2016.

[18] M. I. C. Rachmatullah, J. Santoso, and K. Surendro, "Determining the number of hidden layer and hidden neuron of neural network for wind speed prediction," *PeerJ Comput Sci*, vol. 7, pp. 1–19, 2021, doi: 10.7717/PEERJ-CS.724.

[19] J. D. J. Rubio, "Stability Analysis of the Modified Levenberg-Marquardt Algorithm for the Artificial Neural Network Training," *IEEE Trans Neural Netw Learn Syst*, vol. 32, no. 8, pp. 3510–3524, Aug. 2021, doi: 10.1109/TNNLS.2020.3015200.

[20] G. Luo, L. Zou, Z. Wang, C. Lv, J. Ou, and Y. Huang, "A novel kinematic parameters calibration method for industrial robot based on Levenberg-Marquardt and Differential Evolution hybrid algorithm," *Robot Comput Integr Manuf*, vol. 71, Oct. 2021, doi: 10.1016/J.RCIM.2021.102165.

[21] Z. Yan, S. Zhong, L. Lin, and Z. Cui, "Adaptive Levenberg–Marquardt Algorithm: A New Optimization Strategy for Levenberg–Marquardt Neural Networks," *Mathematics 2021, Vol. 9, Page 2176*, vol. 9, no. 17, p. 2176, Sep. 2021, doi: 10.3390/MATH9172176.

[22] S. Voutsinas, D. Karolidis, I. Voyiatzis, and M. Samarakou, "Development of a multi-output feed-forward neural network for fault detection in Photovoltaic Systems," *Energy Reports*, vol. 8, pp. 33–42, Nov. 2022, doi: 10.1016/J.EGYR.2022.06.107.

[23] M. A. Soyer, N. Tüzün, Ö. Karakaş, and F. Berto, "An investigation of artificial neural network structure and its effects on the estimation of the low-cycle fatigue parameters of various steels," *Fatigue Fract Eng Mater Struct*, vol. 46, no. 8, pp. 2929–2948, Aug. 2023, doi: 10.1111/ffe.14054.

[24] Z. Khandezamin, M. Naderan, and M. J. Rashti, "Detection and classification of breast cancer using logistic regression feature selection and GMDH classifier," *J Biomed Inform*, vol. 111, p. 103591, Nov. 2020, doi: 10.1016/J.JBI.2020.103591.

[25] D. Chhachhiya, A. Sharma, and M. Gupta, "Case Study on Classification of Glass using Neural Network Tool in MATLAB," 2014.

[26] M. Adil, R. Ullah, S. Noor, and N. Gohar, "Effect of number of neurons and layers in an artificial neural network for generalized concrete mix design," *Neural Comput Appl*, vol. 34, no. 11, pp. 8355–8363, Jun. 2022, doi: 10.1007/s00521-020-05305-8.

[27] V. Kaleeswaran, S. Dhamodharavadhani, and R. Rathipriya, "A Comparative Study of Activation Functions and Training Algorithm of NAR Neural Network for Crop Prediction," in *Proceedings of the 4th International Conference on Electronics, Communication and Aerospace Technology, ICECA 2020*, Institute of Electrical and Electronics Engineers Inc., Nov. 2020, pp. 1073–1077. doi: 10.1109/ICECA49313.2020.9297469.

[28] Z. Laabid, A. Moumen, K. Mansouri, and A. Siadat, "Numerical study of the speed's response of the various intelligent models using the tansig, logsig and purelin activation functions in different layers of artificial neural network," *IAES International Journal of Artificial Intelligence*, vol. 12, no. 1, pp. 155–161, Mar. 2023, doi: 10.11591/IJAI.V12.I1.PP155-161.

[29] S. Namasudra, S. Dhamodharavadhani, and R. Rathipriya, "Nonlinear Neural Network Based Forecasting Model for Predicting COVID-19 Cases," *Neural Process Lett*, vol. 55, no. 1, pp. 171–191, Feb. 2023, doi: 10.1007/s11063-021-10495-w.

[30] T. T. Le, "Surrogate neural network model for prediction of load-bearing capacity of cfss members considering loading eccentricity," *Applied Sciences (Switzerland)*, vol. 10, no. 10, May 2020, doi: 10.3390/app10103452.

Open Access This chapter is licensed under the terms of the Creative Commons Attribution-NonCommercial 4.0 International License (http://creativecommons.org/licenses/by-nc/4.0/), which permits any noncommercial use, sharing, adaptation, distribution and reproduction in any medium or format, as long as you give appropriate credit to the original author(s) and the source, provide a link to the Creative Commons license and indicate if changes were made.

The images or other third party material in this chapter are included in the chapter's Creative Commons license, unless indicated otherwise in a credit line to the material. If material is not included in the chapter's Creative Commons license and your intended use is not permitted by statutory regulation or exceeds the permitted use, you will need to obtain permission directly from the copyright holder.